Inorganic Chemistry

Article

pubs.acs.org/IC

Two New Crystals in $Li_mCs_nB_{m+n}O_{2(m+n)}$ ($m + n = 5, 7; m > n$) Series: Noncentrosymmetric $Li_5Cs_2B_7O_{14}$ and Centrosymmetric $Li_4CsB_5O_{10}$

Lin Li,[†,‡] Shujuan Han,[*,†] Binghua Lei,[†,‡] Xiaoyu Dong,[†,‡] Hongping Wu,[†] Zhongxiang Zhou,[†] Zhihua Yang,[*,†] and Shilie Pan[*,†]

[†]Key Laboratory of Functional Materials and Devices for Special Environments, Xinjiang Technical Institute of Physics & Chemistry, Chinese Academy of Sciences, No. 40-1, Beijing South Road, Urumuqi 830011, China

[‡]University of Chinese Academy of Sciences, Yuquan Road, 19, Beijing 100049, China

Supporting Information

ABSTRACT: With the introduction of an alkali metal into the B−O framework, two new alkali metal borate crystals, $Li_5Cs_2B_7O_{14}$ and $Li_4CsB_5O_{10}$, have been obtained for the first time. Both compounds obey a general formula of $Li_mCs_nB_{m+n}O_{2(m+n)}$ ($m + n = 5, 7; m > n$). The two crystals have different three-dimensional (3D) framework structures composed by LiO_n ($n = 4, 5$), CsO_{10}, BO_3, and BO_4 units. $Li_5Cs_2B_7O_{14}$ crystallizes into the polar and noncentrosymmetric space group *Ama*2, while $Li_4CsB_5O_{10}$ belongs to the nonpolar and centrosymmetric space group $P2_1/c$. Detailed structure comparison analysis indicates that the different arrangements of the anionic groups in $Li_mCs_{7-m}B_7O_{14}$ ($m = 4, 5$) and $Li_mCs_{5-m}B_5O_{10}$ ($m = 3, 4$) may arise from the cation size effects, bond-valence requirements, and differences of coordination environment. In addition, in order to get better understandings of electronic structures and linear optical properties, we also carried out first-principle theoretical studies.

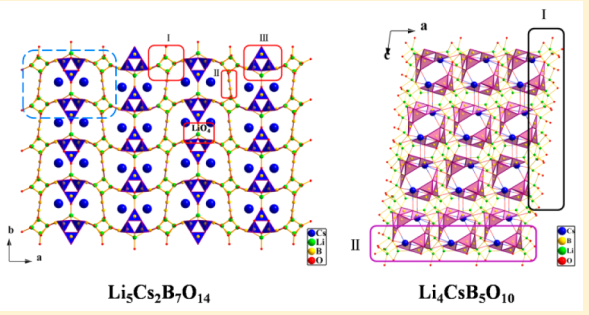

1. INTRODUCTION

Intense interest has been focused on the borates crystals since they have abundant structures and promising technical applications for many advanced technology fields, especially the nonlinear optical (NLO) field.[1−8] As an UV NLO material, it should contain moderate second harmonic generation (SHG) coefficients, a short cutoff edge, and so on.[9−11] Until now, through the great efforts of many scientists, some NLO borate crystals with the aforementioned outstanding performances have been produced.[12−16]

In order to explore new NLO crystals, many methods were put forward.[17−20] The most important and successful method is the cation substitution to inherit the primary perfect properties and overcome shortcomings.[18,19] For example, $RBe_2BO_3F_2$ (R = K, Rb, and Cs)[21] are isostructural but show different NLO properties. It is known to all that the cations with similar size, coordinate environment, and bond valence can be mutually replaced while the host crystal structure remains unchanged. However, it is a particularly difficult challenge to realize the substitution between the cations whose atomic radii have large difference. In the $Li_2O−Cs_2O−B_2O_3$ system, the famous one is $CsLiB_6O_{10}$ (CLBO) owing to its excellent NLO properties for UV applications,[15] but $CsMB_6O_{10}$ (M = Na, K, Rb) species have not been obtained, which may be attributed to the different cation size, various coordinate environment, and diverse reaction condition between Li and M. Owing to these differences, there are few reports on the structural analysis and theoretical calculations among similar compounds containing Li and M. In addition, there are few outstanding compounds reported in this system. Hence, in recent years, we have been focusing on the research of the $Li_2O−Cs_2O−B_2O_3$ system to develop new NLO borate crystals. After many efforts, a series of alkali metal borate crystals were successfully synthesized in our group, such as $Li_3Cs_2B_5O_{10}$[22a] and $Li_4Cs_3B_7O_{14}$,[22b] all of which exhibit a short cutoff edge in the UV region and measurable NLO effects. So, it is meaningful to continue an investigation into the $Li_2O−Cs_2O−B_2O_3$ system and expect to develop new crystals, investigating the structural and NLO properties in this system.

Through our systematic research, two new alkali metal borate crystals, noncentrosymmetric $Li_5Cs_2B_7O_{14}$ and centrosymmetric $Li_4CsB_5O_{10}$, were discovered. Here, comparison of the structures between $Li_5Cs_2B_7O_{14}$ and $Li_4Cs_3B_7O_{14}$,[22b] and $Li_4CsB_5O_{10}$ and $Li_3Cs_2B_5O_{10}$,[22a] is discussed in detail. In view of the above analysis, it can be found that these four compounds follow the chemical formula $Li_mCs_nB_{m+n}O_{2(m+n)}$ ($m + n = 5, 7; m > n$). On the basis of cationic size effects, bond-valence theory, and coordination preferences, substitution of Li and Cs cations influences the arrangement of BO groups, and thereby determines the materials' macroscopic polarity. In addition, characterizations including thermal behavior, spectra, and electronic band structure of $Li_4CsB_5O_{10}$ are also reported.

Received: April 24, 2015
Published: July 21, 2015

DOI: 10.1021/acs.inorgchem.5b00926
Inorg. Chem. 2015, 54, 7381−7387

2. EXPERIMENTAL SECTION

2.1. Reagents. Li_2CO_3 (98.0%), H_3BO_3 (99.5%), $BaCO_3$ (99.0%), and PbO (99.0%) were purchased from the Tianjin Reagent Factory. Cs_2CO_3 (99.5%) was purchased from Institute of Xinjiang metal.

2.2. Preparations of the Two Crystals. $Li_5Cs_2B_7O_{14}$ was obtained from the high temperature solution with $BaCO_3$−PbO as the flux. Starting materials, Li_2CO_3, Cs_2CO_3, H_3BO_3, $BaCO_3$, and PbO at the mole ratio of 7:3:20:1:3, were mixed in a Pt crucible and heated in the vertical furnace to 750 °C, holding at 750 °C for 12 h to make the solution become transparent. The temperature was then decreased to 700 °C rapidly. After that, a Pt wire was dipped into the solution, and the solution was cooled at a slow rate of 2 °C h^{-1} to 600 °C; during the process of cooling, some small crystals were formed around the Pt wire. After the growth was completed, the Pt wire was drawn out from the solution. Afterward, the temperature was lowered at a rate of 20 °C h^{-1} to 30 °C. In the end, except for $Li_5Cs_2B_7O_{14}$, small amounts of $LiBa_2B_5O_{10}$ and PbO were also obtained during the process of growth (Figure S1a in the Supporting Information).

Similarly, $Li_4CsB_5O_{10}$ was also obtained by the spontaneous nucleation method using the flux of H_3BO_3. Starting materials of Li_2CO_3, H_3BO_3, and Cs_2CO_3 (the mole ratio is 8:21:2) were put into a Pt crucible placed in the center of a vertical furnace. The temperature was heated to 800 °C, kept at 800 °C for 12 h, and then lowered to 630 °C rapidly. After this, it was lowered at a slow rate of 2 °C/h to 530 °C; finally, the power to furnace is turned off.

2.3. Powder Synthesis. Powder samples of $Li_5Cs_2B_7O_{14}$ and $Li_4CsB_5O_{10}$ were obtained via the traditional solid state reaction techniques. Although many efforts were made to synthesize $Li_5Cs_2B_7O_{14}$ at various temperatures, we were not able to obtain the material, but $Li_4Cs_3B_7O_{14}$ was synthesized instead (Figure S1b in the Supporting Information). It can be found that when the temperature was increased to 580 °C, $Li_4Cs_3B_7O_{14}$ was obtained. Also, with the increase of the temperature, $Li_4Cs_3B_7O_{14}$ disappeared.

To $Li_4CsB_5O_{10}$, a stoichiometric ratio of Li_2CO_3, H_3BO_3, and Cs_2CO_3 was preheated at 610 °C for 48 h with several intermediate grindings. The powder XRD data were collected on a Bruker D2 PHASER diffractometer at room temperature with Cu Ka radiation (λ = 1.5418 Å). The 2θ range was 10−70° with a step size of 0.02° and a fixed counting time of 1s/step (Figure S2 in the Supporting Information).

2.4. Structure Analysis. Single crystals of $Li_5Cs_2B_7O_{14}$ and $Li_4CsB_5O_{10}$ in the sizes 0.204 × 0.156 × 0.138 mm^3 and 0.208 × 0.159 × 0.102 mm^3, respectively, were fixed on a thin glass fiber for the structure analysis. Data were collected at 296(2) K with monochromatic Mo Kα radiation (λ = 0.710 73 Å), integrating with the SAINT program.[23] The calculation was completed using the SHELXTL crystallographic software package.[24] SHELXS-97[25] was used to solve the structure. PLATON[26] was used to check the structural symmetry. Table 1 summarized the structure refinement information and crystal data. Final atomic coordinates and equivalent parameters are given in Tables S1 and S2 in the Supporting Information. Some bond distances (Å) and angles (deg) for $Li_5Cs_2B_7O_{14}$ and $Li_4CsB_5O_{10}$ are selected and listed in Tables S3 and S4 in the Supporting Information.

2.5. IR Spectrum. The IR spectrum of $Li_4CsB_5O_{10}$ was measured with the Shimadzu Affinity-1 Fourier transform IR spectrometer ranging from 400 to 4000 cm^{-1} using dried KBr reference pellet.

2.6. UV−Vis−NIR Diffuse Reflectance Spectrum. The measurement of the diffuse reflectance spectrum was performed with the (3700DUV) Shimadzu spectrophotometer at room temperature. Data were collected over the range from 190 to 2500 nm. Also, the reflectance spectrum was transformed into absorbance using the Kubelka−Munk function.[27,28]

2.7. Thermal Analysis. The melting behavior of $Li_4CsB_5O_{10}$ was measured in the flowing N_2 atmosphere using a NETZSCH STA 449C thermal analyzer instrument. The measurement temperature range is 25−1200 °C, and heating rate is 10 °C/min.

2.8. Calculational Description. On the basis of the density functional theory (DFT), the CASTEP[29] package was employed to calculate the optical performance and electronic structure of $Li_4CsB_5O_{10}$ and $Li_3Cs_2B_5O_{10}$ involved for comparison. After a battery of successful algorithms, the Ceperley and Alder−Perdew−Zungerof (CA-PZ) functional based on the local density approximation (LDA) and ultrasoft pseudopotential (USP) were chosen as the exchange−correlation functional and pseudopotential. The optimized valence electronic configurations for USP are Li, $1s^22s^1$; Cs, $5s^25p^66s^1$; B, $2s^22p^1$; and O, $2s^22p^4$, respectively. During the calculation, the Broyden−Fletcher−Goldfarb−Shanno (BFGS) minimization technique was employed in geometry optimization, and the converged criteria are that the residual forces on the atoms, the substitution of atoms, and the energy change were less than 0.01 eV /Å, 5× 10^{-4} Å, and 5.0 × 10^{-6} eV per atom, respectively. For $Li_4CsB_5O_{10}$ and $Li_3Cs_2B_5O_{10}$, the energy cutoff of the plane wave basis set and a separation of Monkhorst−Pack k-point sampling both were 380 eV and 0.03/Å, respectively, but the Brillouin zone comprised 5 × 4 × 2 and 6 × 6 × 3 accordingly. The other calculation parameters and convergent criteria were set as the default values of the CASTEP code.

Table 1. Crystal Data and Structure Refinement of the Two Crystals

	$Li_5Cs_2B_7O_{14}$	$Li_4CsB_5O_{10}$
fw	600.19	374.72
T (K)	296(2)	296(2)
λ (Å)	0.710 73	0.710 73
cryst syst	orthorhombic	monoclinic
space group, Z	*Ama*2, 4	$P2_1/c$, 4
unit cell dimensions	a = 21.2775(17) Å	a = 6.894(5) Å
	b = 13.6296(11) Å	b = 9.369(6) Å, β = 98.271(9)°
	c = 4.4283(4) Å	c = 16.004(11) Å
V (Å^3)	1284.22(19)	1022.9(12)
D_c (g cm^{-3})	3.104	2.433
μ (mm^{-1})	5.754	3.655
F(000)	1088	688
2θ range for data collection (deg)	1.91−27.42	2.53−27.52
reflns collected/unique	10 180/1495 [R_{int} = 0.0360]	6119/2333 [R_{int} = 0.0446]
completeness to θ	100.00%	99.20%
GOF on F^2	1.045	1.043
final R indices [$F_o^2 > 2\sigma(F_o^2)$][a]	R1 = 0.0192, wR2 = 0.0429	R1 = 0.0412, wR2 = 0.0879
R indices (all data)[a]	R1 = 0.0219, wR2 = 0.0443	R1 = 0.0621, wR2 = 0.0979
absolute structure param	−0.05(2)	
largest diff peak and hole (e Å^{-3})	0.675 and −0.464	1.702 and −1.657

[a] R1 = $\sum||F_o| - |F_c||/\sum|F_o|$ and wR2 = $[\sum w(F_o^2 - F_c^2)^2/\sum wF_o^4]^{1/2}$ for $F_o^2 > 2\sigma(F_o^2)$.

3. DISCUSSION

3.1. Structures. *3.1.1. Structure of $Li_5Cs_2B_7O_{14}$.* Crystallographic analysis reveals that $Li_5Cs_2B_7O_{14}$ owns the orthorhombic, polar space group *Ama*2. There are 16 atoms consisting of three Li atoms, one Cs atom, four B atoms, and eight O atoms (Table S1 in the Supporting Information) in the asymmetric unit. It exhibits a 3D network which consists of LiO_n (n = 4, 5), CsO_{10}, BO_3, and BO_4 units. In $Li_5Cs_2B_7O_{14}$, there is an interesting feature: the structure contains three kinds of 1D chains (Figure 1). Among these chains, chain I is composed of $Li(3)O_5$ and $Li(2)O_5$ groups (Figure 1a), chain II is formed by the $B(3)O_3$ groups (Figure 1b), and chain III is composed of B_5O_{12} units, which consist of one B_3O_6 ring and two $B(1)O_3$ groups by sharing O(7) and O(8) atoms (Figure

DOI: 10.1021/acs.inorgchem.5b00926
Inorg. Chem. 2015, 54, 7381−7387

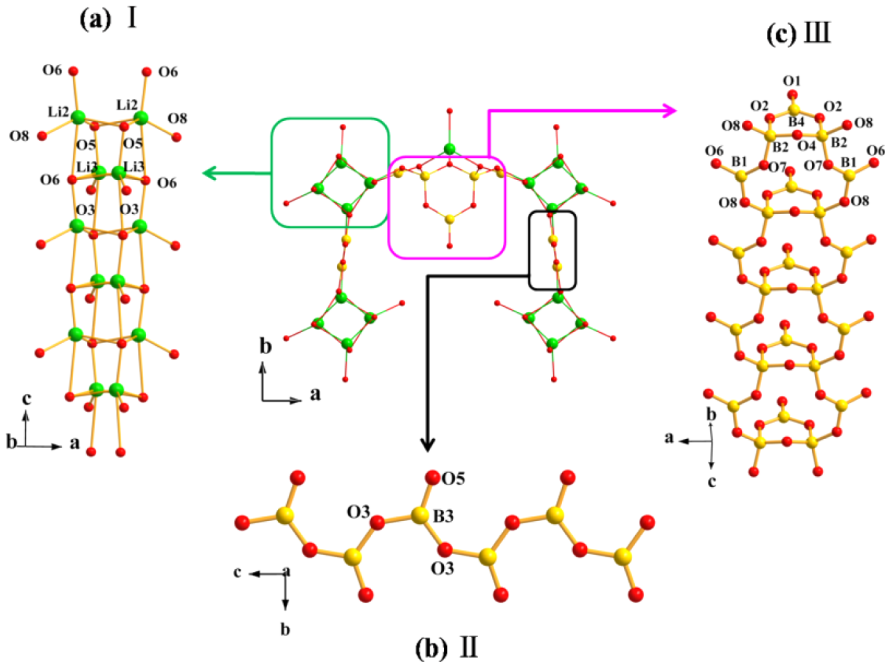

Figure 1. (a) Chain built by Li−O units along *c* axis, (b) chain composed of the BO_3 groups along *c* axis, and (c) chain composed by the B_5O_{12} units.

1c). The three types of 1D chains and isolated $Li(1)O_4$ groups are linked together to build the 3D network with the Cs atoms staying in the cavities (Figure 2).

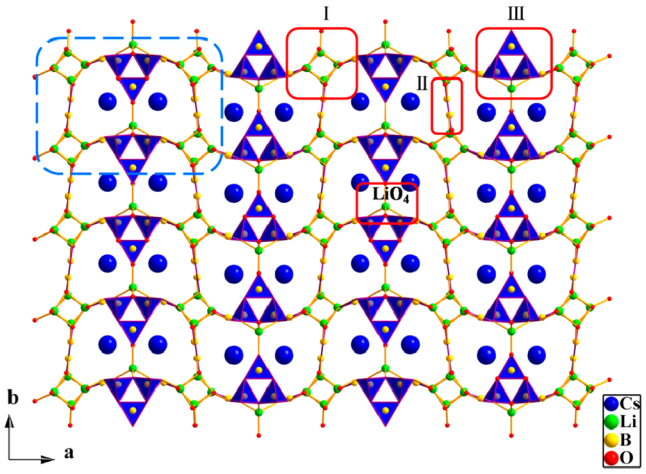

Figure 2. Structure of $Li_5Cs_2B_7O_{14}$.

In $Li_5Cs_2B_7O_{14}$, the Li atoms possess two types of coordination environments. The Li(1) atom is coordinated by four O atoms, forming isolated LiO_4 tetrahedra with Li−O lengths 1.925(18)−1.966(9) Å (av = 1.946 Å). Different from Li(1), other Li atoms, Li(2) and Li(3), are linked to five O atoms with Li−O bond distances 1.900(13)−2.552(13) Å (av = 2.226 Å) and 1.918(11)−2.564(6) Å (av = 2.241 Å), respectively (Table S3 in the Supporting Information). The $Li(2)O_5$ and $Li(3)O_5$ units are joined together via O(5) and O(6) to build a 1D chain (Figure 1a). The Cs atom is surrounded by 10 O atoms, forming the CsO_{10} polyhedron with Cs−O bond distances 3.043(9)−3.512(2) Å (av = 3.278 Å) (Table S3 in the Supporting Information). In $Li_5Cs_2B_7O_{14}$, the CsO_{10} polyhedra are connected together via O to build the 2D layer along the *b* axis (Figure S3 in the Supporting Information). To the B atoms, the B(1), B(3), and B(4) atoms are bonded to three O atoms, building the BO_3 triangulars, while the B(2) atom is connected with four O atoms. In the triangles, the B−O bonds lengths vary from 1.322(5) to 1.424(10) Å (av = 1.373 Å). Also, in the distorted $B(2)O_4$ tetrahedra, the distances are from 1.457(4) to 1.504(6) Å (Table S3 in the Supporting Information). Compared with other borates, the bond lengths and angles are reasonable.[30]

3.1.2. Structure of $Li_4CsB_5O_{10}$. $Li_4CsB_5O_{10}$ belongs to the monoclinic crystal system with a centrosymmetric space group $P2_1/c$. Its asymmetric unit contains 4 unique Li atoms, 1 unique Cs atom, 5 unique B atoms, and 10 unique O atoms (Table S2 in the Supporting Information). In the structure, two types of chains (I and II in Figure 3) and isolated B_5O_{10} groups construct a 3D network. The two types of chains are built by the LiO_n (n = 4, 5) and CsO_{10} groups, respectively (Figure 3a,b). Chain I is formed by LiO_4 and LiO_5 groups interconnected via two O(8) atoms. The bond distances of Li−O in the $Li(1)O_5$, $Li(2)O_5$, $Li(3)O_4$, and $Li(4)O_4$ groups are from 1.944(9)−2.192(8), 1.878(9)−2.440(9), 1.860(9)−2.127(9), and 1.848(9)−2.242(9) Å, respectively (Table S4 in the Supporting Information). The CsO_{10} polyhedra build another 1D chain II extending along the *a* axis via edge-sharing (Figure 3b). The bond distances of Cs−O vary from 2.986(3) to 3.638(4) Å (av = 3.267 Å) (Table S4 in the Supporting Information). The two chains almost vertically arrange to form the 3D network (Figure 3d). The isolated B_5O_{10} units are in the diagonal arrangement to insert into the 3D framework (Figure 3d). The B atoms possess two coordination environments, located in the 3-fold and 4-fold coordination number, respectively. B(1), B(3), B(4), and B(5) are bonded to three O atoms, and the B−O bond lengths are in the range 1.305(6)−1.427(6) Å (av = 1.366 Å), while the B−O bond lengths in the $B(2)O_4$ tetrahedron vary from 1.446(6) to 1.485(6) Å (av = 1.476 Å) (Table S4 in the Supporting Information). Also, all of the values are normal in the BO_3 triangle or BO_4 tetrahedron.[30]

DOI: 10.1021/acs.inorgchem.5b00926
Inorg. Chem. 2015, 54, 7381−7387

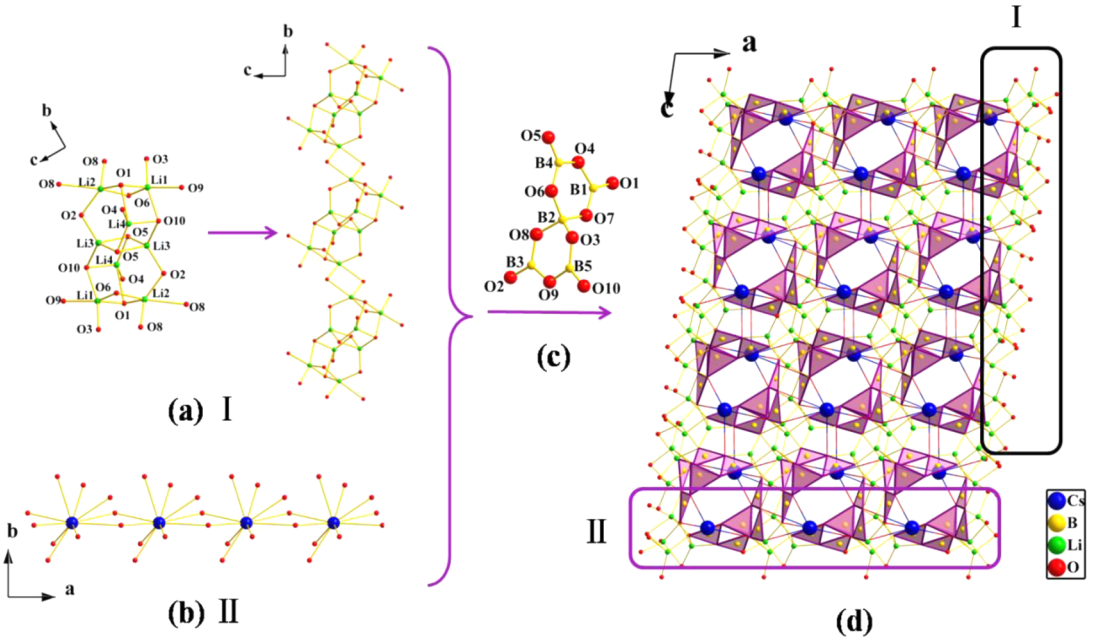

Figure 3. (a) Chain composed of Li−O groups, (b) chain composed of CsO_{10} groups, (c) isolated B_5O_{10} group, and (d) structure of $Li_4CsB_5O_{10}$.

3.1.3. Structural Comparison of $Li_mCs_{7-m}B_7O_{14}$ (m = 4, 5) and $Li_mCs_{5-m}B_5O_{10}$ (m = 3, 4). It is interesting that both $Li_4Cs_3B_7O_{14}$[22b] and $Li_5Cs_2B_7O_{14}$ follow the formula of $Li_mCs_{7-m}B_7O_{14}$ (m = 4, 5); $Li_3Cs_2B_5O_{10}$[22a] and $Li_4CsB_5O_{10}$ follow the formula of $Li_mCs_{5-m}B_5O_{10}$ (m = 3, 4). Among these compounds, only $Li_5Cs_2B_7O_{14}$ is polar, and two are noncentrosymmetric and nonpolar, while $Li_4CsB_5O_{10}$ is centrosymmetric. All of them show the 3D framework composed of LiO_n (n = 4, 5), CsO_n (n = 8, 9, 10), BO_3, and BO_4 units. As for anionic groups, three compounds exhibit a zero-dimensional structure (isolate B_7O_{14} and isolated B_5O_{10} units), while $Li_5Cs_2B_7O_{14}$ shows two types of 1D chains consisting of BO_3 and B_5O_{12} units, respectively (Table 2).

Table 2. Structure Units of Four Compounds

compound	space group	structure units
$Li_4Cs_3B_7O_{14}$[17b]	$P3_12$ (NCS, nonpolar)	isolate B_7O_{14}, LiO_n (n = 4,5), and CsO_n (n = 9, 10)
$Li_5Cs_2B_7O_{14}$	$Ama2$ (NCS, polar)	two chains composed of BO_3 and B_5O_{12} units, respectively, LiO_n (n = 4, 5), and CsO_{10}
$Li_3Cs_2B_5O_{10}$[17a]	$C222_1$ (NCS, nonpolar)	isolate B_5O_{10}, LiO_n (n = 4, 5), and CsO_n (n = 8, 10)
$Li_4CsB_5O_{10}$	$P2_1/c$ (CS)	isolate B_5O_{10}, LiO_n (n = 4, 5), and CsO_{10}

The different structures between $Li_5Cs_2B_7O_{14}$ and $Li_4Cs_3B_7O_{14}$ should originate from the different cation sizes, coordination environment, and the radii of Li and Cs. Compared with the features of the smaller Li atom, the Cs atom has a much larger cation size and higher coordination number (CsO_n (n = 8, 9, 10), LiO_n (n = 4, 5, 6)). With the substitution of the Cs atom, the coordination number will be increased. Compared with the 1D B−O chains, the isolated BO groups have more degrees of freedom in arrangement and provide more terminal O atoms for the Cs atom. Herein, the 1D B−O chains in $Li_5Cs_2B_7O_{14}$ will be destroyed, and the isolated BO groups are produced to accommodate larger Cs atoms in $Li_4Cs_3B_7O_{14}$ (Figure 4). In $Li_4Cs_3B_7O_{14}$, the distorted $Cs(1)O_9$ (av = 3.3068 Å) and $Cs(2)O_{10}$ (av = 3.3896 Å) polyhedra form a 3D network,[22b] while in $Li_5Cs_2B_7O_{14}$, CsO_{10} (av = 3.278 Å) polyhedra form a 2D layer structure (Figure S3 in the Supporting Information). Moreover, both $Li_4Cs_3B_7O_{14}$ and $Li_5Cs_2B_7O_{14}$ contain the LiO_n (n = 4, 5) groups; in $Li_4Cs_3B_7O_{14}$, the Li−O bond distances of $Li(2)O_5$ range from 1.899(11) to 2.369(11) Å (av = 2.099 Å), which are smaller than those in $Li_5Cs_2B_7O_{14}$ (1.900(13)−2.564(6) Å (av = 2.232 Å)). Compared with Cs−O, Li−O shows more covalent properties, influencing the total polarity of the material. In all, under the influence of cation sizes and coordination environment, the polarities for $Li_5Cs_2B_7O_{14}$ and $Li_4Cs_3B_7O_{14}$ change from polar to nonpolar.

For $Li_3Cs_2B_5O_{10}$ and $Li_4CsB_5O_{10}$, owing to the substitution between Li and Cs, their crystal structures are also changed. In $Li_3Cs_2B_5O_{10}$, the distance Cs(1)−Cs(2) is 4.667 Å, which is smaller than that in $Li_4CsB_5O_{10}$ (6.257 Å). Moreover, the CsO_{10} polyhedra form a 1D chain in $Li_4CsB_5O_{10}$ (Figure 3), while the CsO_n (n = 8, 10) polyhedra built a 3D network in $Li_3Cs_2B_5O_{10}$.[22a] Also, in $Li_4CsB_5O_{10}$, the LiO_n (n = 4, 5) polyhedra build a 1D chain via sharing edges (Figure 3); differently, in $Li_3Cs_2B_5O_{10}$, the $Li(1)O_5$ and $Li(2)O_4$ polyhedra are connected through edge-sharing to construct a 2D layer.[22a] From $Li_4CsB_5O_{10}$ to $Li_3Cs_2B_5O_{10}$,[22a] for the excessively large Cs^+ cation, the arrangement of the isolated B_5O_{10} group is changed (from Figure 5a to Figure 5b). Further, in $Li_4CsB_5O_{10}$, this arrangement causes the B_5O_{10} groups to be centrosymmetric, reducing the possibility of crystallizing in the noncentrosymmetric structure. Conclusively, substitution of the cations can change the arrangement of anion groups, and influence the overall structure of the crystal.

3.1.4. Relationship of Formulas. Compared among $Li_5Cs_2B_7O_{14}$, $Li_4CsB_5O_{10}$, and the reported compounds, $Li_3Cs_2B_5O_{10}$, $Li_4Cs_3B_7O_{14}$, there is a certain relationship in their chemical formulas which can be simplified to $Li_mCs_nB_{m+n}O_{2(m+n)}$ ($m + n$ = 5, 7; $m > n$). As reported in ref 31 when $n = m - 1$, the compounds, $Li_mM_nB_{m+n}O_{2(m+n)}$, belong to a topologically related family; however, in $Li_4CsB_5O_{10}$, the fundamental building block is also the isolated B_5O_{10} group,

DOI: 10.1021/acs.inorgchem.5b00926
Inorg. Chem. 2015, 54, 7381−7387

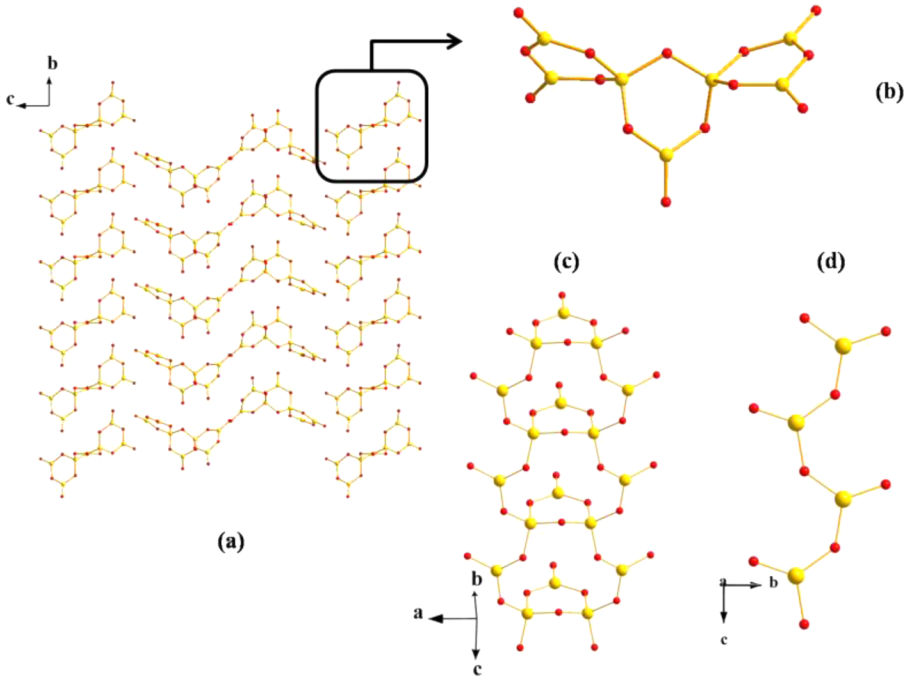

Figure 4. (a) Arrangement of isolated B_7O_{14} groups in $Li_4Cs_3B_7O_{14}$, (b) isolated B_7O_{14} group of $Li_4Cs_3B_7O_{14}$, (c) chain composed of B_5O_{12} in $Li_5Cs_2B_7O_{14}$, (d) chain formed by the BO_3 groups in the structure of $Li_5Cs_2B_7O_{14}$.

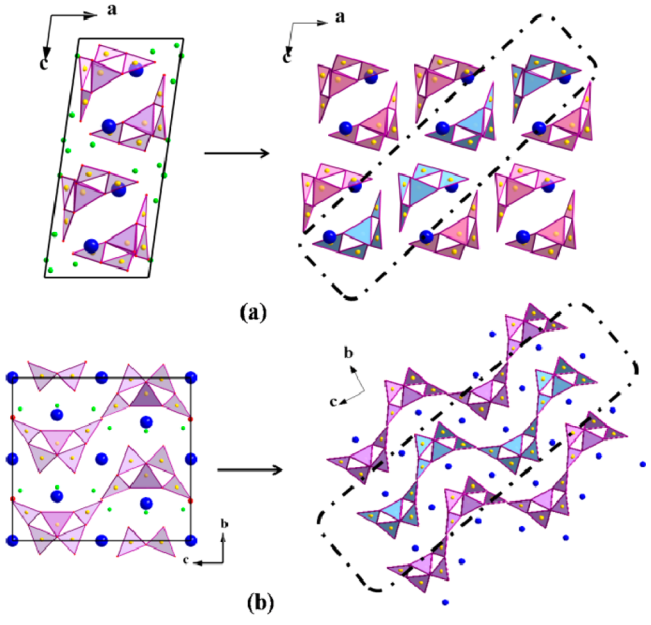

Figure 5. (a) Unit cell and [Cs−B−O] framework of $Li_4CsB_5O_{10}$, and (b) unit cell and [Cs−B−O] framework of $Li_3Cs_2B_5O_{10}$.

which is the same as in $Li_3Cs_2B_5O_{10}$. In $Li_5Cs_2B_7O_{14}$, the connection of the fundamental building blocks changes from the isolated B_7O_{14} groups existing in $Li_4Cs_3B_7O_{14}$ to the 1D chains. It can be speculated that, in $Li_mM_nB_{m+n}O_{2(m+n)}$, when $m + n > 5$ and $n \neq m - 1$, the isolated BO groups may be destroyed, and the 1D chains, 2D layers, and 3D B−O networks are produced.

Considering this regularity, we speculate that a series of new materials possibly exist, such as $Li_6CsB_7O_{14}$ et al. On the basis of the above analysis, the molar ratio of Cs/B (following the same formula, $Li_mCs_nB_{m+n}O_{2(m+n)}$) will influence the linking style, the arrangement of anion groups, and the transformation of macroscopic polarity. Meanwhile, the isomorphism compounds containing Rb also follow this regularity.

3.2. IR Measurement. IR spectrum of $Li_4CsB_5O_{10}$ was measured (Figure S4 in the Supporting Information). The two absorption peaks around 1250 cm^{-1} in the curve are attributed to asymmetric stretching of BO_3 groups. The peaks at 1047 and 930 cm^{-1} can be assigned to the asymmetry and symmetry vibration of the BO_4 groups, respectively. The bands observed at 789, 760, and 730 cm^{-1} can originate from the bending modes of BO_3 groups. The peaks observed in this IR spectrum are in agreement with the ones obtained from other borates.[32−34]

3.3. UV−Vis−NIR Diffuse Reflectance Measurement. The diffuse reflectance spectrum of $Li_4CsB_5O_{10}$ is obtained (Figure S5 in the Supporting Information). Obviously, its cutoff edge is below 200 nm. However, there is one small absorption band around 260 nm, which is maybe caused by the impurity from the reagents. Liu et al. also reported a similar situation.[35] Owing to its short cutoff edge in the UV region, the crystal may be used in the deep UV optical area.

3.4. SHG Property. For $Li_5Cs_2B_7O_{14}$, because of its acentric symmetry *Ama*2, the NLO properties were anticipated. The SHG measurement was performed according to the reported papers.[36,37] The SHG response is about $^1/_5$ times that of KDP for $Li_5Cs_2B_7O_{14}$ (55−88 μm particles). The relatively small SHG effect can be explained as follows: On one hand, as mentioned above, small amounts of centrosymmetric $LiBa_2B_5O_{10}$ and PbO were incorporated in the $Li_5Cs_2B_7O_{14}$ powder (Figure S1a in the Supporting Information). On the other hand, the arrangements of B_5O_{12} and BO_3 groups in $Li_5Cs_2B_7O_{14}$ (Figure 2) are not favorable to generate the large SHG effect.

3.5. Thermal Behavior. Figure S6 in the Supporting Information shows the DSC-TG measurement for $Li_4CsB_5O_{10}$. As the sample is heated, two endothermic peaks (656 and 677 °C) can be observed, which suggests that $Li_4CsB_5O_{10}$ melts

DOI: 10.1021/acs.inorgchem.5b00926
Inorg. Chem. 2015, 54, 7381−7387

incongruently. To further prove the melt behavior of $Li_4CsB_5O_{10}$, 1.0 g of $Li_4CsB_5O_{10}$ was heated to 800 °C in the Pt crucible, and rapidly cooled to ambient temperature. The solidified melt was characterized by XRD, and it can be found that the diffraction pattern of the solid product is different from that of the initial pure powder (Figure S2 in the Supporting Information). It further proved that $Li_4CsB_5O_{10}$ melts incongruently.

3.6. Band Structures and Density of States. The band gaps of $Li_4CsB_5O_{10}$ and $Li_3Cs_2B_5O_{10}$ are characterized in Figures S7a and S8a in the Supporting Information. The result suggests that $Li_4CsB_5O_{10}$ has a direct band gap, and the calculated value is 4.55 eV which is a little less than 4.96 eV, the experimental value, while $Li_3Cs_2B_5O_{10}$ has an indirect band gap. The value of the band gap is less than the experimental value of 6.30 eV, namely, 4.56 eV. The differences between the experimental and calculated band gap values are attributed to the discontinuity of exchange-correlation energy.

The partial and total densities of states for the compounds are exhibited in Figures S7b and S8b in the Supporting Information. The partial densities of states of $Li_4CsB_5O_{10}$ and $Li_3Cs_2B_5O_{10}$ show similar electronic characteristics: near the Fermi surface (energy region varying from −10 to 0 eV), 2p orbitals of O atom are the main contributor. However, at the bottom of the conduction bands, the main occupants are Cs 5p orbitals. From the PDOS calculations, one can see that the interaction between Cs 5p and O 2p orbitals dominated the band gaps of two compounds. However, the different coordination environment of Cs^+ in this two compounds causes different band gaps. For linear optical properties, the birefringence of $Li_4CsB_5O_{10}$ is small (Figure S9 in the SI), which indicates that it is not suitable to be used as a birefringence material.

4. CONCLUSION

In the $Li_2O-Cs_2O-B_2O_3$ system, two new crystals, non-centrosymmetric $Li_5Cs_2B_7O_{14}$ and centrosymmetric $Li_4CsB_5O_{10}$, which are in the $Li_mCs_nB_{m+n}O_{2(m+n)}$ ($m + n = 5, 7$; $m > n$) series, have been successfully synthesized. After structural analyses, it can be found that the coordination environment and arrangement of cations have an important influence on determining the arrangement of anionic groups and crystal structures. In detail, the isolated B_7O_{14} groups are found in $Li_4Cs_3B_7O_{14}$, while the isolated B_7O_{14} groups turn into two 1D chains in $Li_5Cs_2B_7O_{14}$. Both $Li_3Cs_2B_5O_{10}$ and $Li_4CsB_5O_{10}$ consist of the similar structural building units, isolated B_5O_{10}; however, the various arrangements of isolated B_5O_{10} units make $Li_3Cs_2B_5O_{10}$ and $Li_4CsB_5O_{10}$ crystallize into the different space groups, $C222_1$ and $P2_1/c$, respectively. The short UV cutoff edge of $Li_4CsB_5O_{10}$ indicates that it has potential applications in the deep UV area. In the future, research on other compounds of the $Li_mCs_nB_{m+n}O_{2(m+n)}$ series is in progress.

■ ASSOCIATED CONTENT

Supporting Information

CIF files. Detailed single crystal data, bond-valence calculations, powder X-ray data, the 2D layer extending in (010) plane formed by the CsO_{10} polyhedra in $Li_5Cs_2B_7O_{14}$, the 2D layer extending in (010) plane formed by the CsO_{10} polyhedra in $Li_5Cs_2B_7O_{14}$, IR spectrum of $Li_4CsB_5O_{10}$, UV−vis−NIR diffuse-reflectance spectrum of $Li_4CsB_5O_{10}$, DSC-TG of $Li_4CsB_5O_{10}$, calculated band structures, partial and full density of states, and birefringence. The Supporting Information is available free of charge on the ACS Publications website at DOI: 10.1021/acs.inorgchem.5b00926.

■ AUTHOR INFORMATION

Corresponding Authors

*E-mail: hansj@ms.xjb.ac.cn.
*E-mail: zhyang@ms.xjb.ac.cn.
*E-mail: slpan@ms.xjb.ac.cn. Phone: (86)991-3674558. Fax: (86)991-3838957.

Notes

The authors declare no competing financial interest.

■ ACKNOWLEDGMENTS

This work was completed with the support of the Special Fund for Xinjiang Key Laboratories (Grant 2014KL009), the NSFC (Grants 51302307, 51425206), High Level Professional and Technical Personnel of Autonomous Region, Western Light of Chinese Academy of Sciences (Grant XBBS201220), the National Key Basic Research Program of China (Grant 2014CB648400), the Xinjiang International Science & Technology Cooperation Program (20146001), and the Funds for Creative Cross & Cooperation Teams of CAS.

■ REFERENCES

(1) (a) Becker, P. *Adv. Mater.* **1998**, *10*, 979−992. (b) Becker, P.; Frohlich, R. *Z. Naturforsch, B* **2004**, *59*, 256−258.

(2) (a) Huppertz, H.; von der Eltz, B. *J. Am. Chem. Soc.* **2002**, *124*, 9376−9377. (b) Neumair, S. C.; Knyrim, J. S.; Oeckler, O.; Glaum, R.; Kaindl, R.; Stalder, R.; Huppertz, H. *Chem. - Eur. J.* **2010**, *16*, 13659−13670. (c) Mcmillen, C.; Heyward, C.; Giesber, H.; Kolis, J. *J. Solid State Chem.* **2011**, *184*, 2966−2971.

(3) (a) Mao, J. G.; Jiang, H. L.; Fang, K. *Inorg. Chem.* **2008**, *47*, 8498−8510. (b) Zhang, J. H.; Hu, C. L.; Xu, X.; Kong, F.; Mao, J. G. *Inorg. Chem.* **2011**, *50*, 1973−1982. (c) Yang, B. P.; Hu, C. L.; Xu, X.; Huang, C.; Mao, J. G. *Inorg. Chem.* **2013**, *52*, 5378−5384.

(4) (a) Cong, R. H.; Yang, T.; Lin, Z. S.; Bai, L.; Ju, J.; Liao, F. H.; Wang, Y. X.; Lin, J. H. *J. Mater. Chem.* **2012**, *22*, 17934−17941. (b) Lu, P. C.; Wang, Y. X.; Lin, J. H.; You, L. P. *Chem. Commun.* **2001**, *13*, 1178−1179. (c) Li, L. Y.; Li, G. B.; Wang, Y. X.; Liao, F. H.; Lin, J. H. *Chem. Mater.* **2005**, *17*, 4174−4180.

(5) (a) Ok, K. M.; Chi, E. O.; Halasyamani, P. S. *Chem. Soc. Rev.* **2006**, *35*, 710−717. (b) Huang, H. W.; Yao, J. Y.; Lin, Z. S.; Wang, X. Y.; He, R.; Yao, W. J.; Zhai, N. X.; Chen, C. T. *Angew. Chem., Int. Ed.* **2011**, *50*, 9141−9144. (c) Li, R. K.; Chen, P. *Inorg. Chem.* **2010**, *49*, 1561−1565.

(6) (a) Pan, S. L.; Smit, J. P.; Watkins, B.; Marvel, M. R.; Stern, C. L.; Poeppelmeier, K. R. *J. Am. Chem. Soc.* **2006**, *128*, 11631−11634. (b) Yu, H. W.; Pan, S. L.; Wu, H. P.; Zhao, W. W.; Zhang, F. F.; Li, H. Y.; Yang, Z. H. *J. Mater. Chem.* **2012**, *22*, 2105−2100. (c) Pan, S. L.; Wu, Y. C.; Fu, P. Z.; Zhang, G. C.; Li, Z. H.; Du, C. X.; Chen, C. T. *Chem. Mater.* **2003**, *15*, 2218−2221. (d) Yang, Y.; Pan, S. L.; Hou, X. L.; Wang, C. Y.; Poeppelmeier, K. R.; Chen, Z. H.; Wu, H. P.; Zhou, Z. X. *J. Mater. Chem.* **2011**, *21*, 2890−2894. (e) Wang, L.; Pan, S. L.; Chang, L. X.; Hu, J. Y.; Yu, H. W. *Inorg. Chem.* **2012**, *51*, 1852−1858.

(7) (a) Wang, S. C.; Ye, N.; Li, W.; Zhao, D. *J. Am. Chem. Soc.* **2010**, *132*, 8779−8786. (b) Wang, S. C.; Ye, N. *J. Am. Chem. Soc.* **2011**, *133*, 11458−11461.

(8) (a) Hu, Z. G.; Yoshimura, M.; Muramatsu, K.; Mori, Y.; Sasaki, T. *J. Appl. Phys.* **2002**, *41*, 1131−1133. (b) Chen, G. J.; Wu, Y. C.; Fu, P. Z. *J. Cryst. Growth* **2006**, *292*, 449−453.

(9) (a) Wei, Q.; Cheng, J. W.; He, C.; Yang, G. Y. *Inorg. Chem.* **2014**, *53*, 11757−11763. (b) Wang, J. H.; Wei, Q.; Cheng, J. W.; He, H.; Yang, B. F.; Yang, G. Y. *Chem. Commun.* **2015**, *51*, 5066−5068. (c) Rong, C.; Yu, Z.; Wang, Q.; Zheng, S. T.; Pan, C. Y.; Deng, F.; Yang, G. Y. *Inorg. Chem.* **2009**, *48*, 3650−3659.

DOI: 10.1021/acs.inorgchem.5b00926
Inorg. Chem. 2015, 54, 7381−7387

(10) Wu, L.; Sun, J. C.; Zhang, Y.; Jin, S. F.; Kong, Y. F.; Xu, J. J. *Inorg. Chem.* **2010**, *49*, 2715−2720.
(11) (a) Chen, X. A.; Wu, L.; Wang, K.; Chang, X. N.; Xiao, W. Q. *J. Alloys Compd.* **2015**, *623*, 157−163. (b) Reshak, A. H.; Chen, X. A.; Auluck, S.; Kamarudin, H.; Chyský, J.; Wojciechowski, A.; Kityk, I. V. *J. Phys. Chem. B* **2013**, *117*, 14141−14150.
(12) Chen, C. T.; Wu, B. C.; Jiang, A. D.; You, G. *Sci. Sin., Ser. B* **1985**, *28*, 235−243.
(13) Chen, C. T.; Wu, Y. C.; Jiang, A. D.; You, G. M.; Li, R. K.; Lin, S. J. *J. Opt. Soc. Am. B* **1989**, *6*, 616−621.
(14) Wu, Y. C.; Sasaki, T.; Nakai, S.; Yokotani, A.; Tang, H.; Chen, C. T. *Appl. Phys. Lett.* **1993**, *62*, 2614−2615.
(15) Mori, Y.; Kuroda, I.; Nakajima, S.; Sasaki, T.; Nakai, S. *Appl. Phys. Lett.* **1995**, *67*, 1818−1820.
(16) Chen, C. T.; Wang, G. L.; Wang, X. Y.; Xu, Z. Y. *Appl. Phys. B: Lasers Opt.* **2009**, *97*, 9−25.
(17) (a) Zhao, S. G.; Jiang, X. X.; He, R.; Zhang, S. Q.; Sun, Z. H.; Luo, J. H.; Lin, Z. S.; Hong, M. C. *J. Mater. Chem. C* **2013**, *1*, 2906−2912. (b) Zhao, S. G.; Zhang, J.; Zhang, S. Q.; Sun, Z. H.; Lin, Z. S.; Wu, Y. C.; Hong, M. C.; Luo, J. H. *Inorg. Chem.* **2014**, *53*, 2521−2527. (c) Yu, H. W.; Wu, H. P.; Pan, S. L.; Zhang, B. B.; Wen, M.; Yang, Z. H.; Li, H. Y.; Jiang, X. Z. *Eur. J. Inorg. Chem.* **2013**, *32*, 5528−5535.
(18) (a) Marvel, M. R.; Lesage, J. L.; Baek, J.; Halasyamani, P. S.; Stern, C. L.; Poeppelmeier, K. R. *J. Am. Chem. Soc.* **2007**, *129*, 13963−13969. (b) Halasyamani, P. S.; Poeppelmeier, K. R. *Chem. Mater.* **1998**, *10*, 2753−2769. (c) Goodey, J.; Broussard, J.; Halasyamani, P. S. *Chem. Mater.* **2002**, *14*, 3174−3180.
(19) (a) Lee, D. W.; Ok, K. M. *Inorg. Chem.* **2013**, *52*, 5176−5184. (b) Lee, D. W.; Kim, S. B.; Ok, K. M. *Dalton Trans.* **2012**, *41*, 8348−8353.
(20) Cao, X. L.; Hu, C. L.; Xu, X.; Kong, F.; Mao, J. G. *Chem. Commun.* **2013**, *49*, 9965−9967.
(21) (a) Chen, C. T.; Xu, Z. Y.; Deng, D. Q.; Zhang, J.; Wong, G. K. L.; Wu, B. C.; Ye, N.; Tang, D. Y. *Appl. Phys. Lett.* **1996**, *68*, 2930−2932. (b) Wu, B. C.; Tang, D. Y.; Ye, N.; Chen, C. T. *Opt. Mater.* **1996**, *5*, 105−109. (c) Chen, C. T.; Ye, N.; Lin, J.; Jiang, J.; Zeng, W. R.; Wu, B. C. *Adv. Mater.* **1999**, *11*, 1071−1078. (d) Mcmillen, C. D.; Kolis, J. W. *J. Cryst. Growth* **2008**, *310*, 2033−2038.
(22) (a) Yang, Y.; Pan, S. L.; Hou, X. L.; Wang, C.; Poeppelmeier, K. R.; Chen, Z. H.; Wu, H. P.; Zhou, Z. X. *J. Mater. Chem.* **2011**, *21*, 2890−2894. (b) Yang, Y.; Pan, S. L.; Li, H. L.; Han, J.; Chen, Z. H.; Zhao, W. W.; Zhou, Z. X. *Inorg. Chem.* **2011**, *50*, 2415−2419.
(23) *SAINT-Plus, version 6.02A*; Bruker Analytical X-ray Instruments, Inc.: Madison, WI, 2000.
(24) Sheldrick, G. M. *SHELXTL, Version 6.14*; Bruker Analytical X-ray Instruments, Inc.: Madison, WI, 2003.
(25) Sheldrick, G. M. *SHELXTL, version 6.14*; Bruker Analytical X-ray Instruments, Inc., Madison, WI, 2008.
(26) Spek, A. L. *J. Appl. Crystallogr.* **2003**, *36*, 7−13.
(27) Kubelka, P.; Munk, F. Z. *Tech. Phys.* **1931**, *12*, 593−601.
(28) Tauc, J. *Mater. Res. Bull.* **1970**, *5*, 721−730.
(29) Clark, S. J.; Segall, M. D.; Pickard, C. J.; Hasnip, P. J.; Probert, M. J.; Refson, K.; Payne, M. C. *Z. Kristallogr.* **2005**, *220*, 567−570.
(30) (a) Brown, I. D.; Altermatt, D. *Acta Crystallogr., Sect. B: Struct. Sci.* **1985**, *41*, 244−247. (b) Brese, N. E.; O'Keeffe, M. *Acta Crystallogr., Sect. B: Struct. Sci.* **1991**, *47*, 192−197.
(31) Zhang, B. B.; Yang, Z. H.; Yang, Y.; Pan, S. L. *J. Mater. Chem. C* **2014**, *2*, 4133−4141.
(32) Fan, X. Y.; Pan, S. L.; Hou, X. L.; Tian, X. L.; Han, J.; Haag, J.; Poeppelmeier, K. R. *Cryst. Growth Des.* **2010**, *10*, 252−256.
(33) Li, F.; Pan, S. L.; Hou, X. L.; Yao, J. *Cryst. Growth Des.* **2009**, *9*, 4091−4095.
(34) Wang, Y. J.; Pan, S. L.; Hou, X. L.; Zhou, Z. X.; Liu, G.; Wang, J. D.; Jia, D. Z. *Inorg. Chem.* **2009**, *48*, 7800−7804.
(35) Liu, L. J.; Chen, C. T. *J. Cryst. Growth* **2006**, *292*, 472−475.
(36) Kurtz, S. K.; Perry, T. T. *J. Appl. Phys.* **1968**, *39*, 3798−3813.
(37) Fan, X. Y.; Pan, S. L.; Hou, X. L.; Liu, G.; Wang, J. *Inorg. Chem.* **2009**, *48*, 4806−4810.

DOI: 10.1021/acs.inorgchem.5b00926
Inorg. Chem. 2015, 54, 7381−7387